Polymer 51 (2010) 3054–3063

Contents lists available at ScienceDirect

Polymer

journal homepage: www.elsevier.com/locate/polymer

Studies of UV crosslinked poly(*N*-vinylpyrrolidone) hydrogels by FTIR, Raman and solid-state NMR spectroscopies

Xingfeng Zhu [a], Ping Lu [a], Wei Chen [b,c], Jian Dong [a,b,*]

[a] School of Chemistry and Chemical Engineering, Shaoxing University, Shaoxing 312000, China
[b] State Key Laboratory of Coordination Chemistry, Nanjing University, Nanjing 210093, China
[c] Department of Polymer Science and Engineering, Nanjing University, Nanjing 210093, China

ARTICLE INFO

Article history:
Received 7 December 2009
Received in revised form
11 April 2010
Accepted 4 May 2010
Available online 11 May 2010

Keywords:
Hydrogels
Photocrosslinking
Poly(*N*-vinylpyrrolidone)

ABSTRACT

Poly(*N*-vinylpyrrolidone) (PVP) hydrogels have become increasingly important materials for pharmaceutical and biomedical applications. UV-light initiated oxidative crosslinking of PVP represents a novel method for producing PVP based hydrogel materials. However, the mechanism of the gelation by this approach is poorly understood. In this study, the reaction mechanism for the crosslinking process is investigated by FTIR, Raman, and solid-state CP/MAS NMR techniques. Both FTIR and Raman spectra indicate that in the process of free radical oxidative crosslinking, the pyrrolidone ring is partially transformed into a succinimide ring. Solid-state NMR data have confirmed this change, and provided evidence that stable intermediates of 4-hydroperoxy-pyrrolidone (PVP–OOH) and its accompanied 4-hydroxy-pyrrolidone (PVP–OH) are formed. The pyrrolidone hydroperoxide intermediate can account for the efficient crosslinking, producing a sufficient level of macroradicals to form stable hydrogels.

1. Introduction

Hydrogels are water swollen polymer matrices, with a strong capacity to absorb water when placed in aqueous environment. This ability to swell, in physiological conditions, makes it an ideal material for use in drug delivery and immobilization of proteins, peptides, and other biological compounds. Hydrogels with high water content resemble natural living tissue more than any other type of synthetic biomaterial [1,2]. Limited water-absorption capabilities (*ca.* 5–10 wt%) of certain polymeric networks, for example, poly(lactic acid) (PLA), poly(lactide-co-glycolide) (PLGA) and poly(acrylic acid-co-*N*-vinylpyrrolidone), exhibit the ability to retain the drugs for longer periods [3–5].

Poly(*N*-vinylpyrrolidone) (PVP) is capable of binding reversibly to various molecules (dyes, metals and some polymers) in solution, with low cytotoxicity and excellent biocompatibility with living tissue, therefore, PVP often acts as a carrier of some hydrophilic or hydrophobic drugs [6,7] and can be applied for encapsulating DNA and protecting it from intracellular degradation [8]. Chemically crosslinked forms of PVP are also used as disintegrants in pharmaceutical tablets (commercially known as crosslinked polyvinyl pyrrolidone, polyvinyl polypyrrolidone (PVPP), crospovidone, crospolividone [9]), which swell rapidly in water with an appreciable swelling force. They are also used to remove or extract impurities from solutions.

Traditionally, PVP hydrogel networks are formed by copolymerization with a bifunctional monomer or by chemical crosslinking of linear PVP with persulfates or Fenton reagents, i.e., through a redox system [10]. Preparation of PVP gels directly from linear PVP through γ-irradiation (^{60}Co) or electron beam has received considerable attention, due to the advantage that the hydrogels are free of cytotoxic residual monomers [11–13]. More recently, a new procedure by UV light irradiation of linear PVP or its interpolymer complexes have been proposed for such hydrogels [14–21]. The advantages of the UV irradiation technique are manifold, not simply the very low capital outlay *versus* the high-energy γ-ray radiation method, and the extremely short time for reliable gel formation. UV crosslinked PVP hydrogels showed a strong gel mechanical behavior with viscoelastic moduli values similar to those of biological gels [20]. By using the UV irradiation procedure, it is possible to include in the porous hydrogel formulation important components which are photo-resistant, but γ-ray radiation vulnerable, to use as “smart dressing”, which could tune the hydrogel functional properties to specific applications. Early studies of direct UV crosslinking of PVP were complicated by the accompanied photo-degradation reaction, resulting in low yields of the gels [14–16,20]. Recently, hydrogen peroxide was found to

* Corresponding author. School of Chemistry and Chemical Engineering, Shaoxing University, Shaoxing 312000, China. Tel.: +86 575 88342511; fax: +86 575 88341521.
E-mail address: jiandong@usx.edu.cn (J. Dong).

0032-3861/$ – see front matter © 2010 Elsevier Ltd. All rights reserved.
doi:10.1016/j.polymer.2010.05.006

significantly accelerate the crosslinking process of the PVP aqueous solution through effectively suppressing the severe photo-degradation during UV irradiation [17]. In spite of such technical advances and high potential, little is known about the structure and crosslinking mechanisms of the PVP hydrogels generated by UV light irradiation. In this study, we present an experimental investigation on the crosslinking mechanisms of the hydrogels obtained by UV irradiation of PVP-hydrogen peroxide solutions, through complementary spectroscopic analyses. This provides a better description of the material for a more precise relationship between macroscopic function and molecular structure.

2. Experimental

2.1. Materials and method

Analytical grade poly(*N*-vinyl-2-pyrrolidone) (PVP K-30) and aqueous solutions of hydrogen peroxide (30%) were purchased from Sinopharm.

Aqueous PVP solutions with polymer concentrations ranging from 0.5% to 5% wt (5–50 mg mL^{-1}) were found to be effective for crosslinking. Typically, 2.00 g of PVP dissolved in 97.5 mL of water were combined with hydrogen peroxide solution (2.5 mL, 30% concentration). After stirring for 3 h, 10 mL of the solution was transferred into a Petri dish (5 cm i.d.), and put under a UV lamp in a closed dark box. Irradiation was carried out by using a high-pressure UVA Hg lamp with a linear flux of 160 W cm^{-1} (Bluesky Special Lamps Development Co., Ltd, Zhuozhou, China). The emission spectrum of the lamp is featured by a main peak at 360 nm, a weak peak at 254 nm, and a set of secondary peaks in the range of 250–550 nm. The lamp was put at a distance of 20 cm above the reaction dish to achieve the best gelation results to produce 40 mW cm^{-2} of radiant flux.

An irradiation time of 5–50 min, depending on the PVP concentration, was found to be sufficient to obtain high gelation yields. The insoluble gels were thoroughly washed in distilled water for 1 day, separated from the solution, and dried in vacuum at 60 °C for at least 24 h to their constant weights. The average gel fractions (g) was estimated by extraction of 3–4 samples, and calculated from the ratio of the dry gel weight to the initial PVP weight. The sol fractions (s) were calculated as $s = 1 - g$.

2.2. Spectroscopic analysis

FTIR spectra of the final dried gels were recorded on a Thermo Nicolet Nexus 310 FTIR spectrometer at a resolution of 4 cm^{-1}, after 32 scans were co-added. In the FTIR spectroscopic analysis of initial crosslinking process, 100 mg of PVP were dissolved in 20 mL of distilled water, cast on different CaF_2 crystals to form uniform surface films, and dried at 40 °C under vacuum for 24 h H_2O_2 solutions (concentration 0.375%) were added equally onto the PVP thin films, which were subsequently brought under UV light irradiation for a time ranging from 60 s to 600 s, respectively. The exposed films were dried at 40 °C under vacuum for 24 h, and analyzed by FTIR transmission method.

FT-Raman spectra of the dried gel solids were obtained on a Bruker Optics FT-Raman 100 spectrometer, equipped with a 1064 nm Nd-YAG laser and a liquid nitrogen cooled Ge detector. The laser power was set at 100 mW and about 200–1000 scans were co-added to improve S/N ratio. Solid-state NMR experiments were carried out at ambient temperature (25 °C) on a Bruker DSX-300 FT NMR spectrometer operating at a 13C resonance frequency of 75.47 MHz. Samples were analyzed under cross-polarization/magic-angle spinning (CP/MAS) conditions using 4-mm zirconia rotors at a spinning frequency of 5 kHz. A 90° pulse width of 3.8 μs was employed, and the CP Hartmann–Hahn contact time was set at 1.0 ms for all experiments, since the experiment demonstrated that the contact time was suitable for all samples. Sidebands were suppressed by using TOSS pulse sequences during data collection. The chemical shifts of all 13C spectra were externally referenced to the carbon signal of solid adamantane (38.3 ppm relative to TMS).

For vibrational normal mode analysis, full geometry optimization of the model compounds of the polymers, including PVP, polyvinylsuccinimide, hydroxylated PVP compounds, and crosslinked structures, was carried out for the subsequent estimation of harmonic force constants at the density functional theory (DFT) level of B3LYP/6-31 + G(d), i.e., electron correlation effect included Becke's three-parameter exchange functional using the correlation functional of Lee, Yang, and Parr, by using Gaussian 03 software [22]. The absence of imaginary vibrational frequencies confirmed that the optimized geometries correspond to ground-state energy minima, not to saddle points. The raw frequencies were converted by a single scaling factor of 0.985, mainly to correct for the anharmonicity effect and the use of finite basis set.

3. Results and discussion

3.1. UV photocrosslinking of PVP accelerated by hydrogen peroxide

Crosslinked PVP can be prepared by UV irradiation in the presence of hydrogen peroxide. The insoluble hydrogels were obtained with high yields by this method. The conversion rate of the gelation (in weight percentages of the gel fractions g) was found to be almost linear with the UV irradiation time (see Fig. 1). The crosslinked yield gradually reaches a maximum of 80% in about 50 min of UV irradiation. The efficient process is quite comparable to the radical-induced crosslinking of PVP by γ-rays. In contrast, in the absence of H_2O_2, the crosslinking yield under the same condition was found to be almost negligible. Likewise, in the absence of UV irradiation, PVP forms a stable complex with H_2O_2 without forming gels [21,23].

To analyze the ratio of radiation-induced degradation to crosslinking density, Charlesby and Pinner's classical method [24] was first used, which states that

$$s + s^{1/2} = \frac{p_0}{q_0} + \frac{2}{q_0 u D} \tag{1}$$

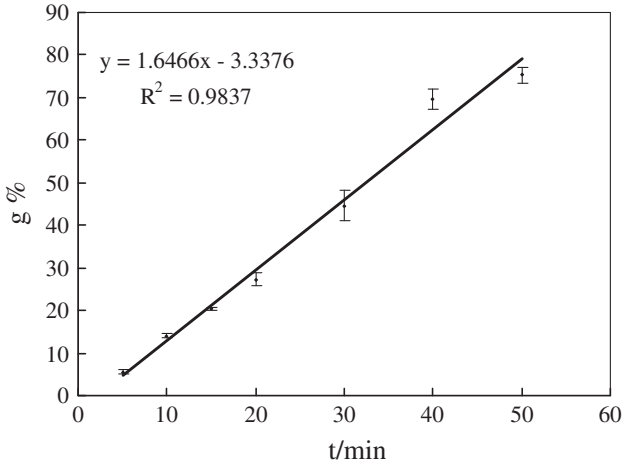

Fig. 1. Dependence of the conversion (gel weight relative to the initial PVP weight in percentages, g%) on the UV irradiation time. A linear relationship was obtained with a regression coefficient of 0.9837 for the first 50 min of crosslinking.

where s is the sol fraction, p_0 is the degradation density (mean value of chain scissions per dose and monomeric unit), q_0 is the crosslinking density (mean value of crosslinks per dose and monomeric unit), D is the applied radiation dose, and u is the polymerization degree. The intercept of $s + s^{1/2}$ *versus* $1/D$ plot is the ratio p_0/q_0 for describing the competition between degradation and crosslinking.

Fig. 2 (top panel) displays the results of the data analysis according to Eq. (1). The deviation in the sol/dose curve from the straight line predicted by Charlesby–Pinner formula is similar to many typical cases found in the crosslinking of polymers by high-energy γ-radiation. This is mainly caused by the departure of the distribution of molecular weight from a pure randomness.

Charlesby–Rosiak approach [25], a more general treatment for the crosslinking process in polymer samples of any initial molecular weight distribution, is given by

$$s + s^{1/2} = \frac{p_0}{q_0} + \left(2 - \frac{p_0}{q_0}\right)\left(\frac{Dv + Dg}{Dv + D}\right) \quad (2)$$

where s, D have the same meanings as in Eq. (1), Dv is the virtual dose (a dose that would be necessary for converting the real sample into a sample of the most probable molecular weight distribution of $M_w/M_n = 2$), Dg, the dose necessary to produce the first insoluble gel fraction. The gelation data were analyzed by finding Dg and Dv values, which provide the best fit according to Eq. (2). As can be seen in Fig. 2 (bottom panel), a reasonably good linear fit in terms of Eq. (2) can be obtained for the experimental data (regression coefficient $R^2 = 0.9136$). We obtained $p_0/q_0 = 0$. Previous studies of UV crosslinking of PVP in the absence of H_2O_2 gave p_0/q_0 values ranging from 0.34 to 0.50 [16,20], while in the presence of H_2O_2 p_0/q_0 values between 0.10 and 0.30 were reported by using a low-pressure UV lamp (with a maximum emission $\lambda_{max} = 254$ nm) [17]. Our data indicated that in the H_2O_2 assisted UV photocrosslinking by a high-pressure lamp (with a main peak at 360 nm), the chain scission or degradation is negligible.

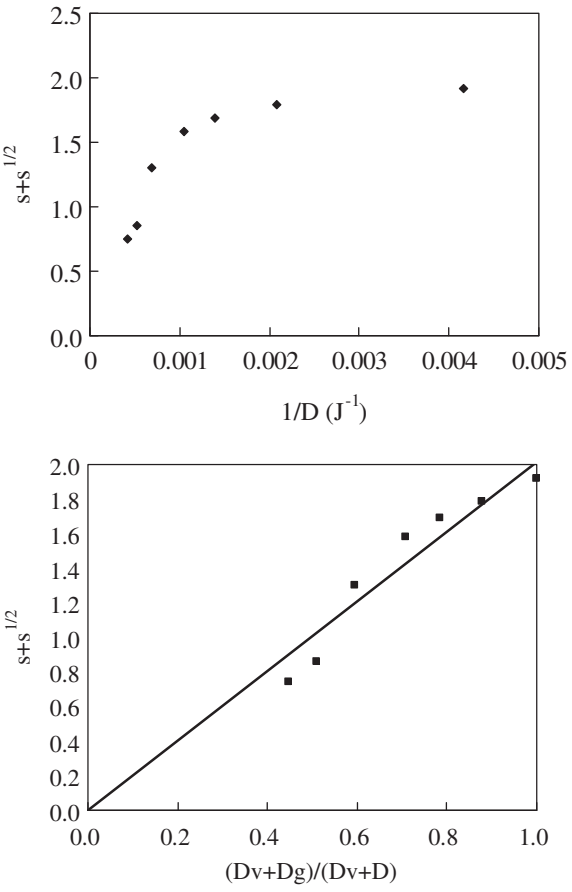

Fig. 2. (Top) Sol/gel data treatment according to classical Charlesby–Pinner relation. (Bottom) data treatment according to Charlesby–Rosiak relation. [PVP] = 20 g L^{-1}, 2.5 mL/100 mL 30% H_2O_2 (20 mM).

3.2. Imidization of the pyrrolidone ring in the crosslinked PVP gel

FTIR spectroscopic analysis of the final dried products surprisingly showed significant changes in the polymer, unlike the γ-ray-induced crosslinking where the predominant changes are the formation of backbone carbon–carbon bonds. As shown in Fig. 3B–D, several new bands are observed in the spectra of the PVP solids crosslinked for 20–40 min, in comparison to the spectrum of the pure PVP solid (Fig. 3A). The bands at 1769 and 1691 cm^{-1} are well resolved near the amide I band of the pyrrolidone ring, which appears at 1670 cm^{-1} in the solid PVP before gelation (Fig. 3A) and shifted downward to around 1657 cm^{-1} in the PVP after gelation. The downshift of the amide I band of the pyrrolidone ring is attributable to the formation of the hydrogen-bonded state of the C=O group to the water and H_2O_2 molecules. Normal mode analysis of PVP based on density functional theory (DFT) was performed and characteristic IR bands are assigned and listed in Table 1. Although the band near 1285 cm^{-1} in the PVP spectrum (Fig. 3A) due to the ring C–N stretching coupled with the ring CH_2 wagging seems to remain in the gel spectrum of Fig. 3D, several new bands have emerged. The new bands at 1769 and 1691 cm^{-1} in Fig. 3D are ascribed to the C=O stretching modes of succinimide rings (see structure in Scheme 1D below) [26], which is verified by Raman spectroscopic analysis (see below). Normal mode analysis of polyvinylsuccinimide model compound also shows that the succinimide ring has a characteristic IR mode near 826 cm^{-1} due to ring CH_2 twisting (see Table 1), which is supported by the appearance of a new band at 820 cm^{-1} in Fig. 3D. Other new spectral features near 1376, 1173, and 1061 cm^{-1} are brought about by partial oxidation of the pyrrolidone ring and concomitant crosslinking. The origin of these bands is discussed below.

In order to confirm the structural changes in early time scale during crosslinking, thin PVP films with H_2O_2 oxidant (about 10 μm thick) were made and subjected to UV irradiation for a short period of time. FTIR spectra collected for the films exposed in the first 10 min of UV irradiation are shown in Fig. 4. As seen in Fig. 4, thin PVP films cast from an aqueous solution display an amide I band near 1660 cm^{-1} and a ring band at 1290 cm^{-1}. The latter becomes less pronounced in the film spectra after UV irradiation for 10 min. The time-dependent increase in the intensity of the new carbonyl bands near 1768 and 1698 cm^{-1} are quite evident in the thin films after UV irradiation, due to the oxidation of the pyrrolidone ring to imide ring. The weak band at 1768 cm^{-1} is due to the symmetric stretching of the imide C=O groups while the strong band at 1698 cm^{-1} is due to the asymmetric stretching of the two C=O groups in the succinimide ring, as proved by our DFT-based normal mode analysis. Changes in the CH_2 groups in the pyrrolidone ring have also led to the reduction of the intensity of the bands in the region between 1490 and 1423 cm^{-1}. Again, new broad peaks near 1373 and 1179 cm^{-1} are observed in the irradiated films. Fig. 4 clearly indicates that oxidation of the pyrrolidone ring occurs quickly in the very early stage of the crosslinking process. This is in contrast to the very slow photooxidation of PVP in the absence of H_2O_2, which occurs only in a time span of about 100–400 h [27].

The formation of the succinimide ring by oxidation of the pyrrolidone side chains is verified by Raman spectroscopy. Fig. 5

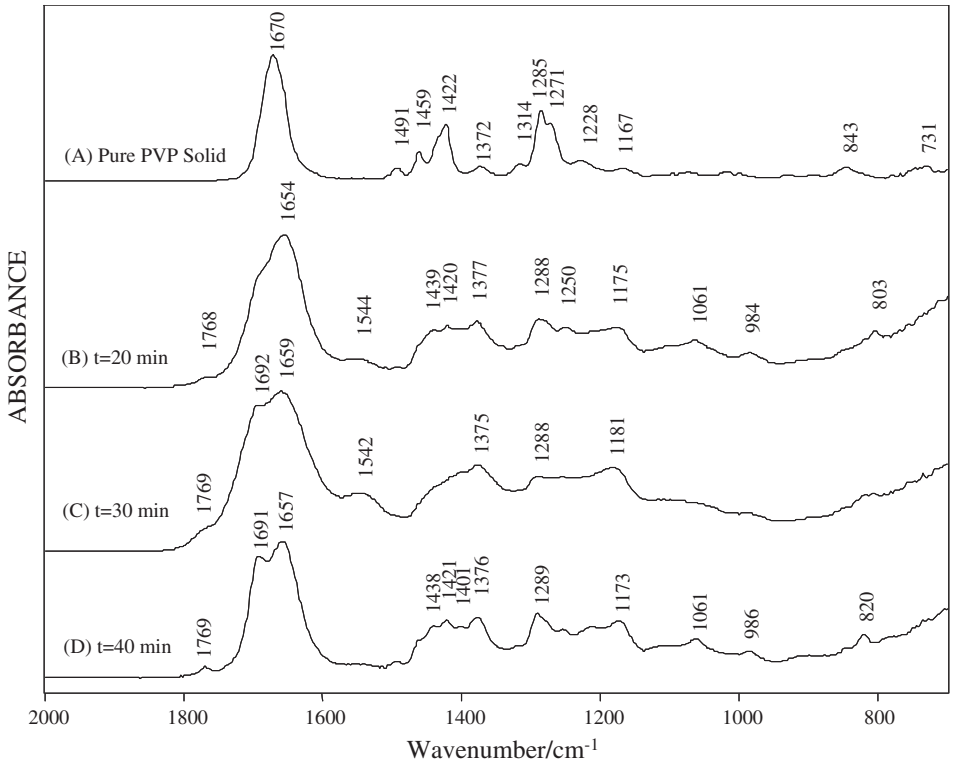

Fig. 3. FTIR spectra of pure PVP solid before gelation (A), and dried PVP gels after UV irradiation for various time (B–D).

Table 1
Characteristic IR bands of PVP, hydroxylated species, polyvinyl succinimide, and two crosslinked structures predicted by DFT-based normal mode analysis.

PVP	PVP–C4OH	PVP–NCOH	polyvinyl succinimide	PVP crosslink structure 1	PVP crosslink structure 2
1451.8 ring CH_2 wag + ring C–N stretch + C–H bend in methine	1423.1 C4–H def. + O–H bend	1416.7 C–N stretch + ring CH_2 wag		1418.1 C–N stretch + C4–H wag adjacent to O	1415.6 C–N stretch + C4–H wag 1404.3 ring CH_2 wag
1384.2 weak, C–H bend in methine + ring CH_2 wag + N–C stretch	1374.9 C4–H wag + methine C–H bend. + C–N stretch	1344.0 N–C stretch + OH bend + ring CH_2 wag	1366.3 ring C–N symmetric stretch	1366.1 strong, C4–H wag adjacent to O	1376.0 strong, C4–H wag adjacent to O
1275.7 C–N stretch + ring CH_2 wag	1264.9 C–N stretch + C4–H wag + ring CH twist + OH bend	1287.8 C–N stretch + ring CH_2 wag	1269.0 ring CH_2 wag	1257.1 ring CH_2 wag + C4–H wag	1280.9 C–N stretch + ring CH_2 wag
1219.2 ring CH_2 twist + N–C stretch	1149.0 ring CH_2 twist	1229.0 C–N stretch + ring CH_2 twist	1213.4 ring C–N asymmetric stretch	1170.1 strong, ring CH_2 twist	1256.4 N–C stretch 1163.4 strong, ring CH_2 twist
1176.7 weak, ring CH_2 twist	1058.8 strong, ring in-plane bend + ring CH_2 twist	1207.1 ring CH_2 twist	1119.1 ring in-plane bend	1052.1 ring CH_2 rock	1055.7 ring CH_2 rock
	985.0 ring in-plane bend	1119.8 OH bend		1033.8 C–O–C asymmetric stretch + ring in-plane def.	1040.9 ring in-plane bend + C–O–C asymmetric stretch
848.0 ring in-plane bend	797.5 ring in-plane bend		825.6 ring CH_2 twist	983.0 strong, C–O–C asymmetric stretch	975.0 strong, C–O–C asymmetric stretch

Note: In the calculation, N-(3′-pentyl)-pyrrolidone, 4-hydroxyl-N-(3′-pentyl)-pyrrolidone, N-(2′-hydroxyl-2′-propyl)-pyrrolidone, and N-(3′-pentyl)-succinimide was used for PVP, C4-hydroylated PVP (PVP–C4OH), methine-hydroxylated PVP (PVP–NCOH), and polyvinylsuccinimide, respectively. The structures of these species in the polymer are illustrated in Scheme 5. For the crosslinked structure 1 shown in Scheme 4, N,N′-dimethyl- substitution was used for calculation; the crosslinked structure 2 is shown in Scheme 4. A total of 78, 87, 63, 75, 87, and 105 normal modes exist for these model compounds of PVP, PVP–C4OH. PVP–NCOH, polyvinylsuccinimde, the crosslink structure 1, and the crosslink structure 2, respectively. Normal modes associated only with C=O stretching and the ring methylene scissoring vibrations which are overlapped with the main chain CH_2 scissoring modes are not listed here.

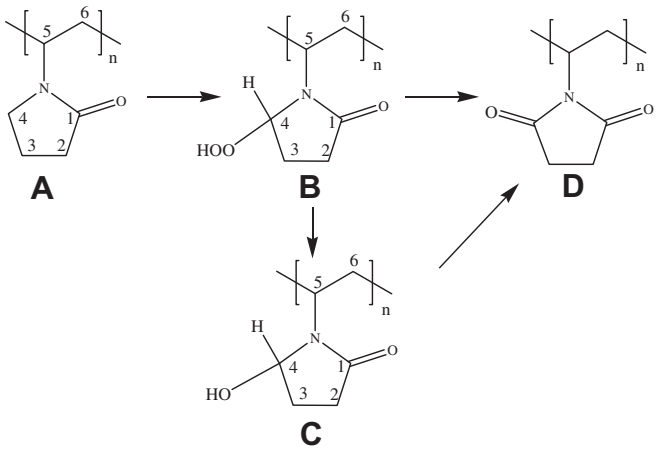

Scheme 1. Reaction pathway for conversion of pyrrolidone ring to succinimide ring.

compares the Raman spectra of the PVP solid before gelation and after gelation. As shown in Fig. 5, a new C═O peak appears at 1769 cm^{-1} in the PVP gels near the original amide I carbonyl peak near 1665 cm^{-1}. This new C═O peak corresponds to the weak 1769 cm^{-1} in the FTIR spectra of the gel very well. The symmetric stretching of the succinimide's two C═O groups has led to the appearance of this intense band in the Raman spectra of the gels, whereas the asymmetric stretching of the two C═O groups of the succinimide ring expected at 1690 cm^{-1} (corresponding to a strong band in FTIR near 1691–1698 cm^{-1} in Figs. 3 and 4) is a weak peak in the Raman spectra [26], thus becoming barely observable near the intense 1665 cm^{-1} amide I band of the pyrrolidone ring. Most of the gel spectral features in Fig. 5 seem to be very close to those of the pure PVP solid, indicating conversion of the pyrrolidone ring to the succinimide ring is not complete. Intensity reduction of the pyrrolidone ring breathing mode at 934 cm^{-1} by about 30–40% in the gel spectrum (using the 1442 cm^{-1} band of main chain

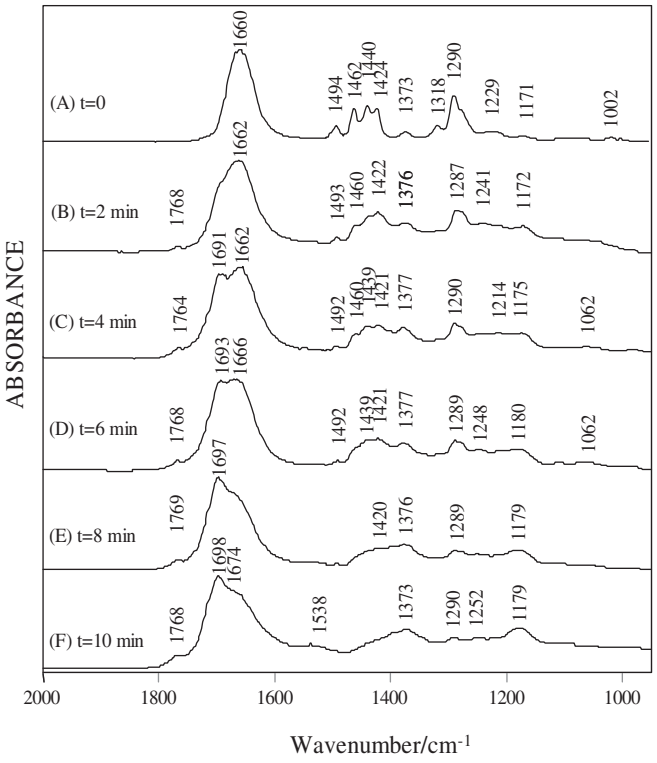

Fig. 4. FTIR spectra of PVP thin films cast on CaF_2 crystals at different UV irradiation time.

methylene deformation as a reference) also implies the partial conversion of the pyrrolidone ring. Moderate changes in the ring modes near 849 and 743 cm^{-1} in the Raman spectrum of Fig. 5C can be ascribed to the presence of the succinimide ring [26].

In order to quantify the amount of the succinimide formed, Raman spectroscopic analysis was performed by measuring the carbonyl

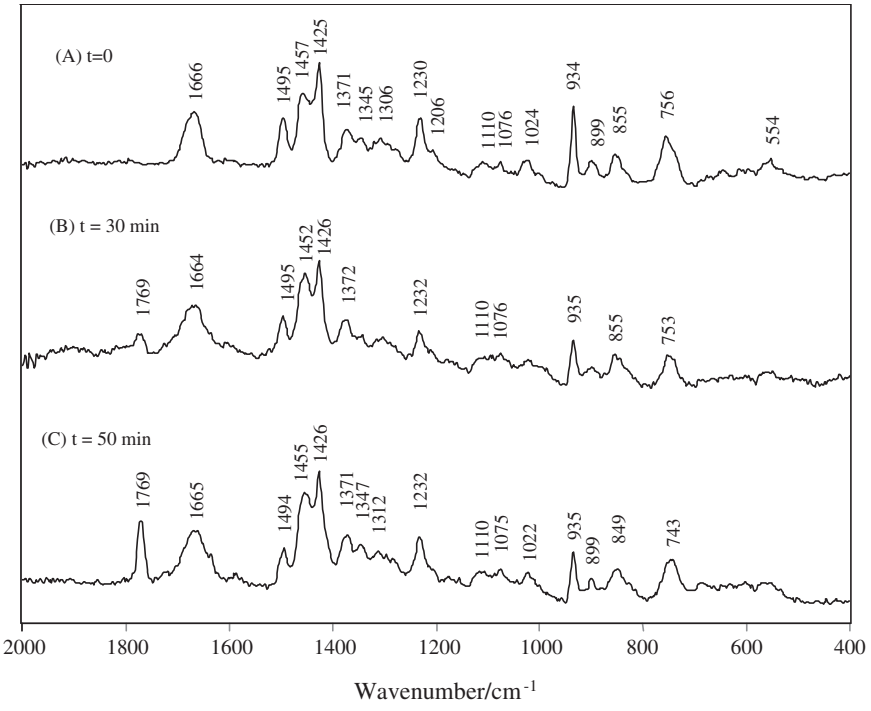

Fig. 5. Raman spectra of the PVP: (A) pure PVP before UV irradiation; (B) dried PVP gels after UV irradiation in H_2O_2 for 30 min and (C) dried PVP gels after UV irradiation for 50 min.

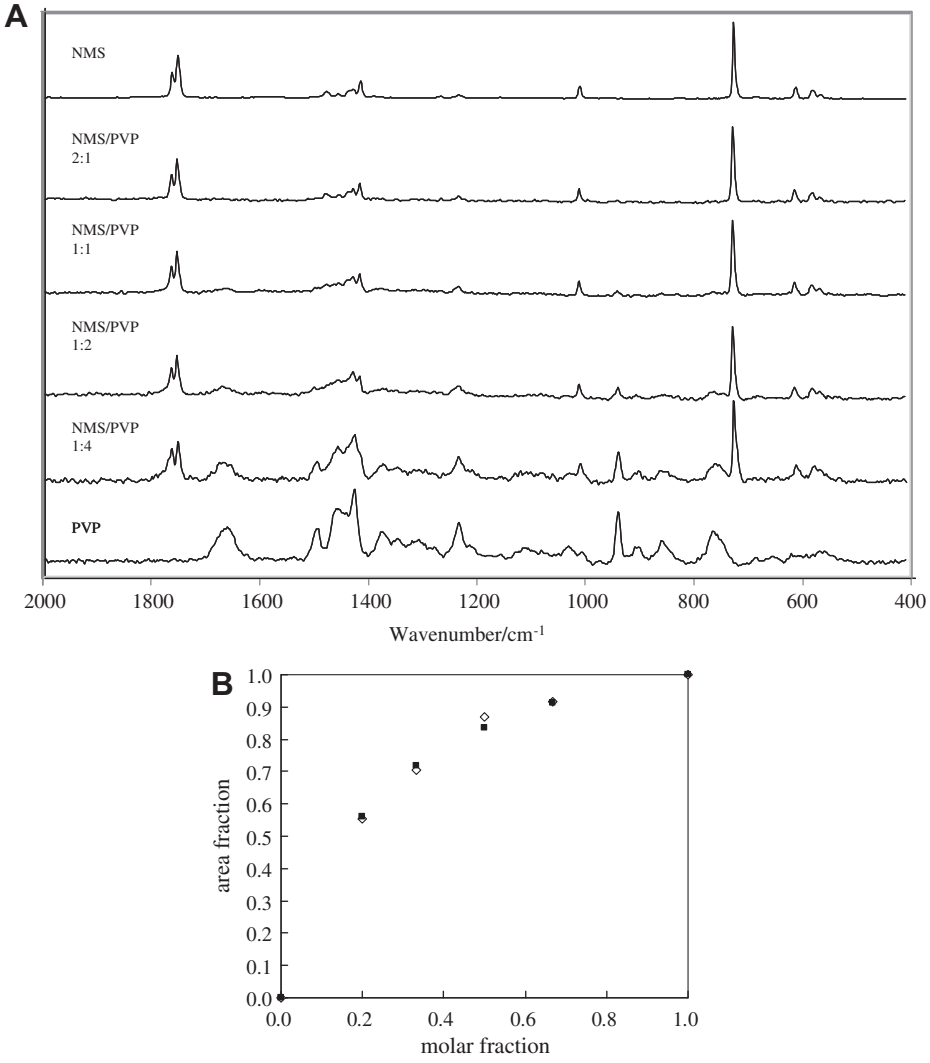

Fig. 6. (A, top panel) Raman spectra of mixtures of *N*-methylsuccinimde and PVP at different molar ratios (the doublet in the C=O band of *N*-methylsuccinimde is due to Fermi resonance). (B, bottom panel) Measured (open diamonds) and calculated (solid squares) succinimide C=O peak fractions in the mixtures.

peak areas in the mixtures of varying compositions of PVP and *N*-methylsuccinimide (Fig. 6A). The peak area fractions y of the imide component in the total C=O peak areas in the mixtures were correlated to the known molar fractions x of the imide (Fig. 6B), and a good nonlinear relationship $y = 5.123x/(4.123x + 1)$ (with a regression coefficient $R^2 = 0.9984$) was obtained from Raman data (which means that the molar scattering coefficient of the imide C=O group is 5.123 times that of the amide group) and used to calculate the molar fractions of the succinimide formed in the crosslinked gels.

The measurement showed that the molar fraction of the succinimide was only 0.105 in the hydrogel made in solution after 50 min irradiation. At such a moderate level of imidization, some changes related to crosslinking groups, such as C–O stretching insensitive in Raman spectra are not visible in Fig. 5. The reason for the appearance of intense bands of the imide C=O moiety in the Raman spectra of Fig. 5 is due to the higher Raman scattering cross-sections (or higher scattering capacity) of the imide C=O stretching vibration than that of the lactam ring's C=O stretching.

The changes in the PVP chains in the gel are studied by CP/MAS solid-state NMR spectroscopy. Fig. 7 compares the scale-expanded C-13 NMR spectra in an overlaid format before irradiation and after irradiation. The NMR spectrum of the gel prepared by prolonged irradiation for 40 min in H_2O_2 is essentially the same as the 20 min irradiation spectrum shown in Fig. 7. Assignments of the peaks are facilitated by a solution NMR study based on 2-dimensional HSQC–TOCSY and TOCSY experiments [28]. Thus, the pyrrolidone ring side-chain's methylene carbons are assigned at δ18.7 ($^3CH_2$), δ31.7 ($^2CH_2$), and δ43.1 ($^4CH_2$) ppm (see numbering in Scheme 1). The main chain methylene carbon signal is assigned to the weak shoulder peak around δ35.7 ppm, while the main chain methine carbon is located at 43–46 ppm and overlapped with the $^4CH_2$ peak at δ43.1 (see Fig. 7B) [28]. The peak at 176.6 ppm is attributed to the carbonyl carbon in the pyrrolidone ring of PVP.

As can be seen in Fig. 7A, the carbonyl carbon peak is shifted from 176.6 ppm to 177.4 ppm after UV irradiation. This kind of shift is expected from the presence of the imide carbonyls formed, which is in perfect agreement with an early NMR study of the oxidation of *N*-methylpyrrolidone compound to *N*-methylsuccinimide [29]. A new shoulder peak is clearly observed near 29.8 ppm in the gel spectrum in Fig. 7B, which is a signal from the CH_2 groups in the newly formed succinimide rings, while the intensity of the pyrrolidone ring's $^3CH_2$ peak at 18.7 ppm relative to the ^2C peak at 31.7 ppm or the carbonyl peak is reduced in Fig. 7B after crosslinking; these changes are consistent with the partial conversion of the $^3CH_2$ group in the pyrrolidone ring to the CH_2 groups in the succinimide ring [29].

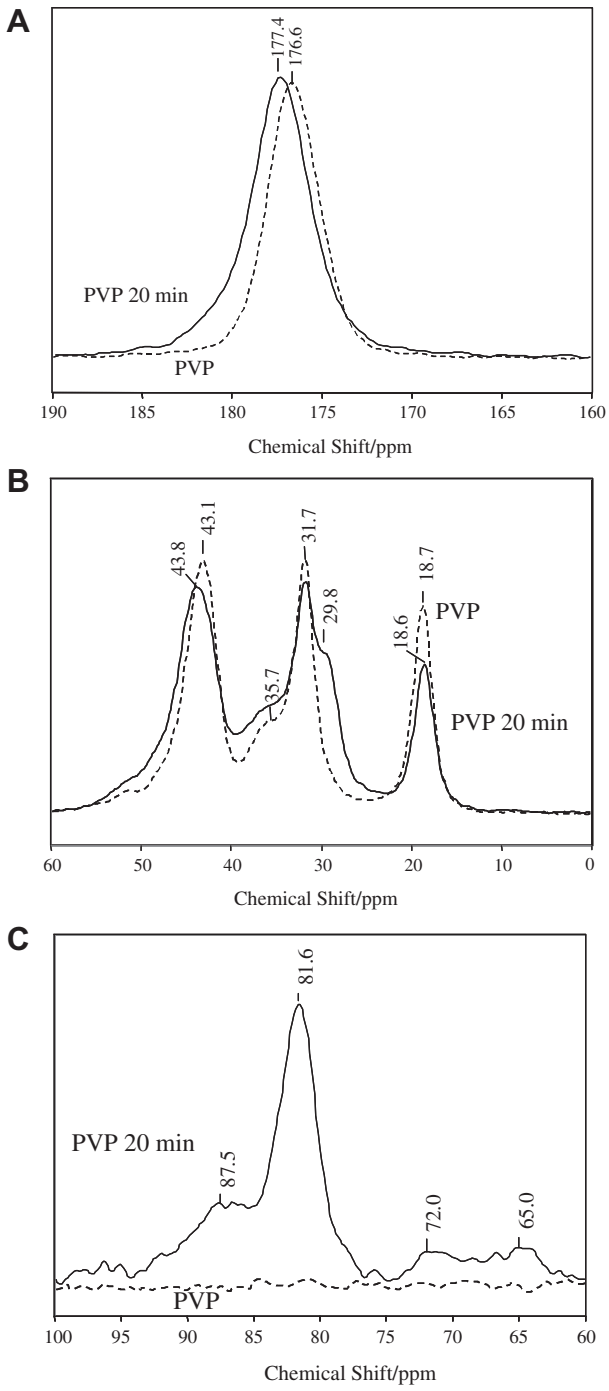

Fig. 7. Overlaid NMR spectra of PVP before gelation (dashed line) and after UV irradiation for 20 min (solid line) in expanded scale.

3.3. Crosslinking of PVP from hydroperoxide intermediate

A new peak at 81.6 ppm in Fig. 7C in the gel spectrum is due to the signal of ^{4}C carbon in hydroxy-pyrrolidone species (PVP–C4OH) (see structure in Scheme 1C). Formation of this kind of hydroxylated species was also observed in the oxidation of the compound *N*-methylpyrrolidone to *N*-methylsuccinimide, which produced a C-13 signal at 83.8 ppm in the same carbon of the hydroxylated intermediate [30], quite close to the resonance position observed here. The calculated chemical shift of the ^{4}C carbon of Scheme 1C obtained by ChemDraw Ultra is at 83.0 ppm, which is consistent with the

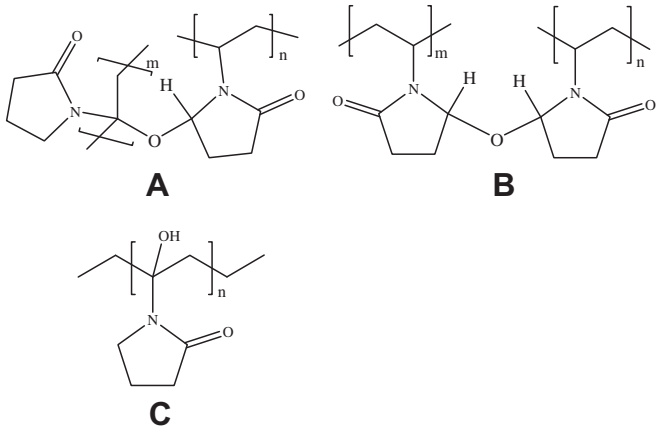

Scheme 2. (A) Crosslinks between methine carbon and hydroperoxy intermediate; (B) crosslinks from the hydroperoxide intermediate rings; and (C) hydroxylation on the methine carbon of the main chain.

observed value. This substitution on the ring leads to new infrared bands near 1060 and 983 cm^{-1} in the FTIR spectra of the gels shown in Fig. 3 (their assignments are discussed below).

The peak at 87.5 ppm in Fig. 7C in the gel spectrum is attributed to the ^{4}C carbon in the hydroperoxide intermediate (PVP–OOH) (see structure in Scheme 1B), since this hydroperoxide intermediate was also observed in the oxidation of *N*-methylpyrrolidone and found to be a stable species [20,30]. The calculated chemical shift of the ^{4}C carbon in the PVP–OOH is 89.8 ppm. In the γ-ray-induced peroxidation of PVP, the PVP–OOH hydroperoxide was so stable that only a few percentages of its concentration were decayed in a period of nearly a month [31].

New peaks at 72 and 65 ppm in the gel spectrum of Fig. 7C, absent in the linear PVP, are due to the ring ^{4}C carbon atom and methine carbon, respectively, that form N–C–O crosslinks from the hydroperoxide intermediate (see structure in Scheme 2A). The calculated chemical shift of the methine carbon that forms a C–O crosslink with PVP–C4OH side chain in Scheme 2A is at 63.5 ppm, while the ring ^{4}C carbon that forms a C–O–C crosslink with a methine carbon is expected to have a chemical shift at 69.6 ppm, as predicted by ChemDraw Ultra. Crosslinks from the hydroperoxide intermediate rings (Scheme 2B) may also contribute to the peak at 72.0 ppm from the ^{4}C atoms, which also forms N-C-O–C-N crosslinks, since the calculated chemical shift for the ^{4}C atoms in Scheme 2B is 71.5 ppm. Hydroxylation of the methine carbon in the PVP main chain (Scheme 2C) is predicted to have a carbon signal near 67.9 ppm. Literature reports on the C-13 NMR studies of *N*-hydroxymethylamides are in good agreement with this assignment [32], thus it is possible that hydroxylation at the methine carbon of Scheme 2C is also present. Multiple peaks centered at 72 ppm and 65 ppm are also clearly observed in the 40 min irradiation spectrum of the dried gel. They are indicators of the crosslinks formed by N–C–O–C bonds shown in Scheme 2A and B.

The presence of such crosslinking bonds is also reflected in the FTIR data in Fig. 3, which showed intense infrared absorption bands near 1376 and 1170–1180 cm^{-1} in the gel spectra. Normal mode analysis results of the crosslinked structures (whose structures are shown in Scheme 4) and hydroxyl intermediates and succinimide (whose structures are shown in Scheme 5), based on the same quantum chemical calculation method as that used for the above PVP model compound (B3LYP/6-31 + G(d) method), are summarized in Table 1 for the intense infrared-active bands. From these analyses, the ether-type crosslinked structure 2 has a strong infrared band at 1376 cm^{-1} due to C–H wagging vibration in its ether moiety >C–O–CH<, while the ether-type crosslinked

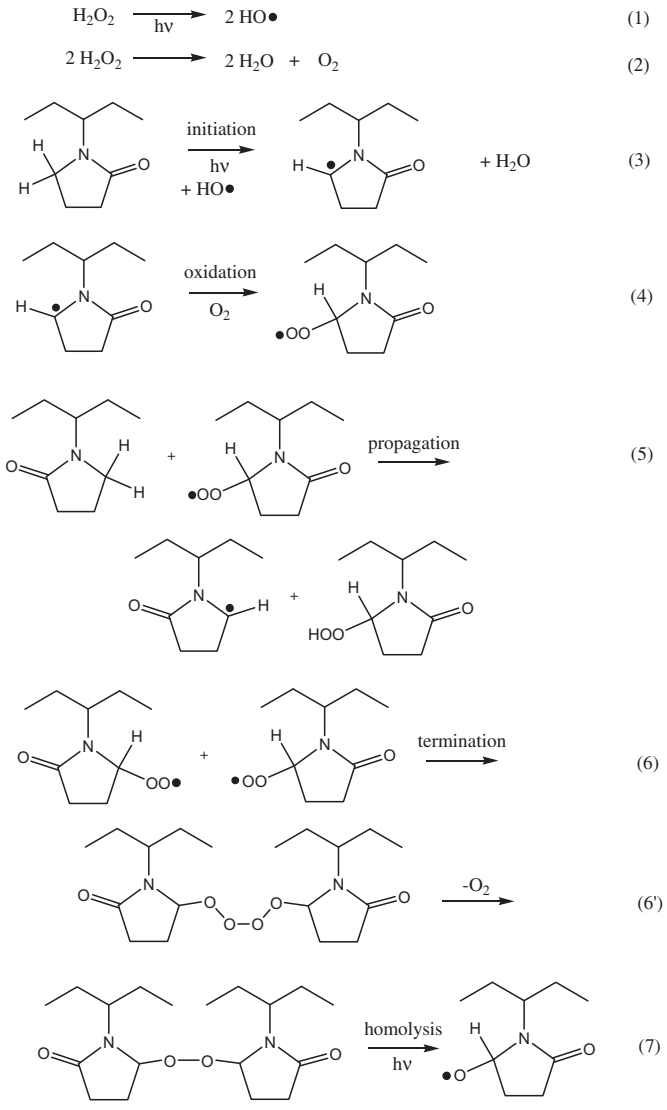

Scheme 3. Reaction mechanism of the formation of hydroperoxide species.

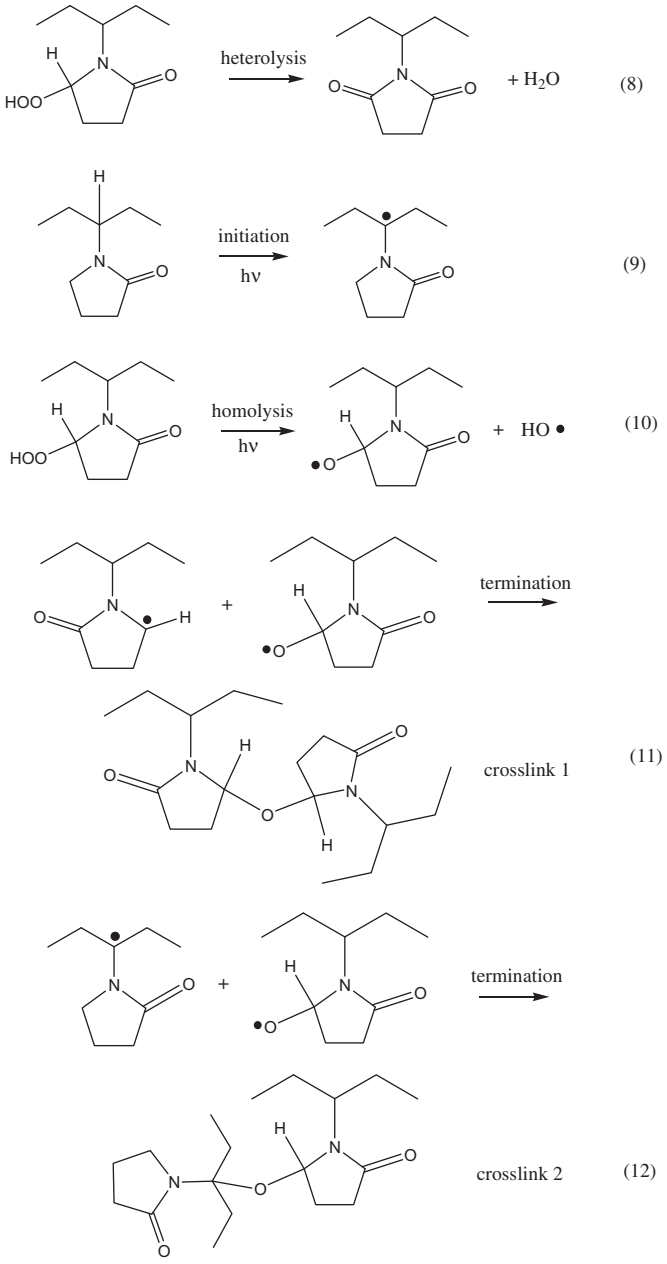

Scheme 4. Reaction mechanism of the formation of succinimide and crosslinks.

structure 1 has a strong infrared band at 1366 cm^{-1} due to C–H wagging vibration in its ether moiety >CH–O–CH<. In addition, the C–O–C crosslinked structures have a strong C–O–C asymmetric stretching mode near 980 cm^{-1}. The IR band at 1173 cm^{-1} is due to ring CH_2 twisting in such crosslinked rings. The band at 1060 cm^{-1} can be attributed to a ring in-plane bending coupled with ring CH_2 twist vibration in the C4-hydroxylated pyrrolidone species and a ring CH_2 rocking vibration in the crosslinked structures. Therefore, all the new IR bands in the gels can be assigned to the crosslinked products (see Scheme 4 for their structures) and the hydroxyl species (see Scheme 5 for their structures), apart from the bands due to the imide group discussed above.

3.4. Reaction pathway for crosslinking initiated by UV

On the basis of the key intermediate species and crosslinks in the above spectroscopic data, a reaction mechanism can be reasonably deduced and explained by comparison with the previous oxidation studies of lactams and *N*-alkylamides. It was reported that pyrrolidone is oxidized more easily than the seven-, eight-, nine- and thirteen-membered lactams as well as linear *N*-alkylamides [33,34]. The high oxidizability of the five- and six-membered lactams can be attributed to the relatively easier homolytic splitting of the *N*-vicinal CH bond and to the different reactivity of lactam radicals in the propagation step of the chain oxidation [33]. Hence, during the oxidation, the pyrrolidone ring can be transformed into a radical with an increased population and lifetime, as compared with other lactams.

The detailed reaction mechanisms for production of the succinimide, hydroperoxide, hydroxide species, and the crosslinks shown in Schemes 1 and 2 are depicted in Schemes 3–5. As is known, the C–H bond in the CH_2 group adjacent to nitrogen is the weakest bond in lactams and *N*-alkylamides [33–38]; thus in the oxidation of pyrrolidone, the UV-light-assisted generation of a macroradical on this CH_2 group is initiation of the reaction (see reaction (3) in Scheme 3). It is very likely that abstraction of H atoms from the N adjacent carbon is achieved by the hydroxyl radicals generated in reaction (1).

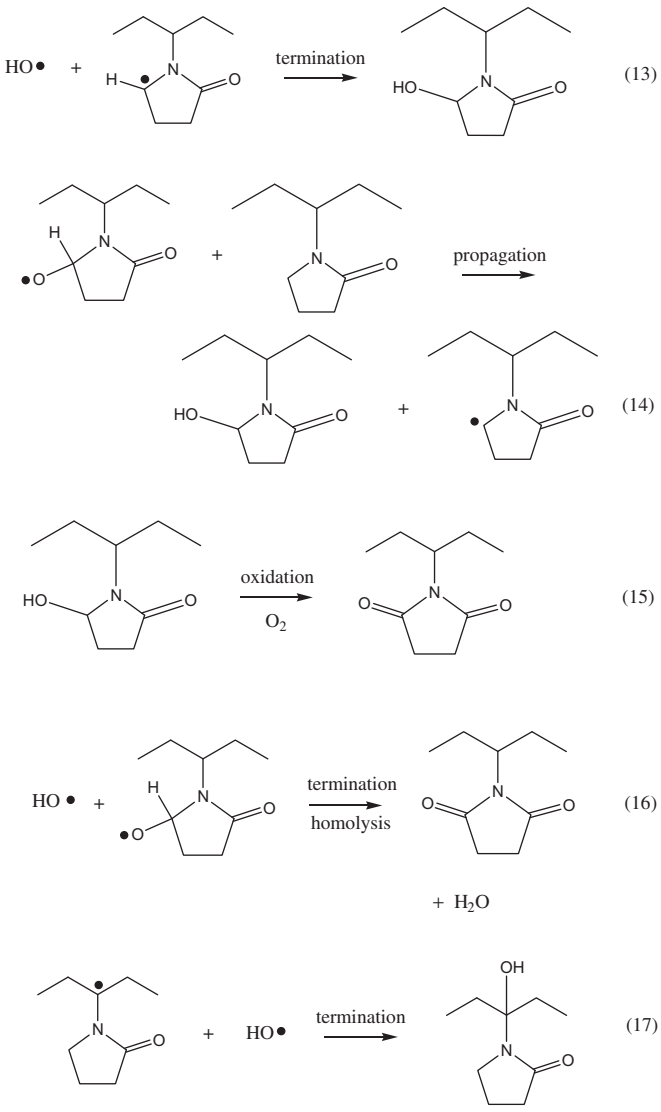

Scheme 5. Reaction mechanism of the formation of hydroxy species and conversion to succinimide.

In the presence of oxygen this alkyl radical is oxidized with practically zero activation energy to the corresponding peroxy radical, as depicted in reaction (4) of Scheme 3. The radical propagation reaction of this peroxy species subsequently yields the oxidation product of the pyrrolidone hydroperoxide (reaction (5) in Scheme 3). The pyrrolidone peroxy radicals are terminated by a bimolecular reaction (reaction (6) in Scheme 3), forming tetraoxygen bridges which are decomposed into peroxy groups and oxygen (reaction (6′) of Scheme 3), and next, homolytically decomposed to alkoxy radicals in reaction (7).

For the pyrrolidone ring oxidation, the rate-limiting process is the abstraction of hydrogen from the pyrrolidone ring producing the corresponding radical. This reaction is involved in both the initiation and the propagation steps of the radical chain oxidation of the pyrrolidone rings.

In the initial phase, the primary oxidation product, hydroperoxide, accumulates in the reaction medium. This is the main oxidation product at the beginning of the reaction. Depending on the experimental conditions, the hydroperoxide begins to decompose. In the oxidation medium where oxygen quenches the radical-induced chain decomposition, the pyrrolidone hydroperoxide can undergo heterolysis to yield a succinimide ring and water (reaction (8) of Scheme 4) and UV-light-assisted homolysis to alkoxy and hydroxy radicals (reaction (10) of Scheme 4).

In the auto-oxidation of lactams and *N*-alkylamides, such homolysis generally is the main source of the initiating radicals [33,34]. It causes the oxidation rate to grow, so that the reaction proceeds into the stage of maximum oxidation rate. During this reaction stage, the concentration of hydroperoxide in the reaction medium continues to grow, and imide is formed by heterolysis. Through intermolecular recombination between the alkoxy radical and the hydrogen-abstracted radical of pyrrolidone (generated from the reaction (3)), the termination reaction produces crosslinks of type 1, as shown in reaction (11). Alternatively, initiation at the methine carbon adjacent to the N atom may be achieved by the hydroxyl radicals generated in reaction (1), resulting in a carbon radical (see reaction (9)), which may also recombine with the alkoxy radical to produce crosslinks of type 2, as shown in reaction (12).

The alkyl radical produces a hydroxy compound species (reaction (13) in Scheme 5). The hydroxy compound may also be generated in a radical propagation reaction from the alkoxy radical species, producing a new alkyl radical of pyrrolidone, as shown in reaction (14) of Scheme 5. In the presence of O_2, the alcohol species undergoes rapid oxidation to *N*-substituted succinimide (reaction (15) in Scheme 5). The succinimide species may also be generated from the alkoxy radical by homolytic scission of C–H bond (reaction (16)). Finally, the hydroxylated species at the methine carbon may be produced by termination with a hydroxyl radical (reaction 17).

Effective gel formation at high yields indicates that intermolecular crosslinking dominates over chain scission/degradation. In the absence of H_2O_2, radicals generated at the methine carbon by UV light (reaction (9)) may result in C–C bond scission, when they are not terminated to form crosslinks of type 2 with alkoxy radicals (reaction (12)). Therefore, a high level of chain scission (degradation) of ~50%–70% were reported [13,19]. In the presence of H_2O_2, the appearance of the alkoxy species generated from the PVP-OOH intermediate in reaction (10) and from the PVP–O–O–PVP peroxide species in reaction (7) quickly form crosslinks of types 1 and 2 (reactions (11) and (12)) in the termination reactions, minimizing the tendency for chain scission.

4. Conclusions

Efficient formation of PVP hydrogels can be realized by direct irradiation using a high-pressure Hg lamp, in the presence of hydrogen peroxide, without significant scission or degradation of the main chain. In the reaction, approximately 10% of the pyrrolidone rings are transformed into succinimide side chains by oxidation. This imidization process involves generation of two kinds of species, pyrrolidone hydroperoxide and pyrrolidone hydroxide. The first hydroperoxide intermediate was formed in the *N*-vicinal C–H bond in the pyrrolidone ring. Further macroradical reactions generate pyrrolidone rings with hydroxyl groups in the *N*-vicinal C atoms. The hydroperoxide and hydroxy species also account for the formation of the succinimide ring. Recombination of the alkoxy macroradicals with the alkyl radicals is responsible for the crosslinking reactions between the oxidized pyrrolidone rings, as well as between the methine carbon and the oxidized pyrrolidone ring.

The PVP hydrogels formed by this process may be used in circumstances where high-energy radiation production is not available, but with an additional advantage that the main chain degradation is avoided.

Acknowledgments

This work was supported by the National Natural Science Foundation of China (No. 20974063), Department of Science and Technology of Zhejiang Province (No. 2009R10040), Department of Education of Zhejiang Province (No. 20070495), State Key Laboratory of Coordination Chemistry, Nanjing University, and Shaoxing University (No. 08LG1005).

References

[1] Lin CC, Metters AT. Adv Drug Deliv Rev 2006;58:1379–408.
[2] Chun MK, Cho CS, Choi HK. J Controlled Release 2002;81:327–34.
[3] O'Hagan DT, Jeffery H, Davis SS. Int J Pharm 1994;103:37–45.
[4] Rafati H, Coombes AGA, Adler J, Holland J, Davis SS. J Controlled Release 1997;43:89–102.
[5] Jin L, Lu P, You H, Chen Q, Dong J. Int J Pharm 2009;37:82–8.
[6] Lopes CMA, Felisberti MI. Biomaterials 2003;24:1279–84.
[7] Brunius CF, Ulrica E, Ann-Christine A. J Polym Sci Pt A: Polym Chem 2002;40:3652–61.
[8] Robinson BV, Sullivan FM, Borzelleca JF, Schwartz SL. PVP: a critical review of kinetics and toxicology of polyvinylpyrrolidone (povidone). MI, USA: Lewis Publishers Inc.; 1990.
[9] Bühler V. Polyvinylpyrrolidone excipients for pharmaceuticals, povidone, crospovidone and Copovidone. Berlin: Springer; 2005.
[10] Barros JAG, Fechine GJM, Alcantara MR, Catalani LH. Polymer 2006;47:8414–9.
[11] Rosiak M, Ulansky P. Radiat Phys Chem 1999;55:139–51.
[12] Can HK. Radiat Phys Chem 2005;72:703–10.
[13] Benamer S, Mahlous M, Boukrif A, Mansouri B, Youcef SL. Nucl Instrum Methods Phys Res B 2006;248:284–90.
[14] Kaczmarek H, Kaminska A, Swiatek M, Rabek JF. Angew Makromol Chem 1998;261/262:109–21.
[15] Kaczmarek H, Szalla A, Kamiska A. Polymer 2001;42:6057–69.
[16] Lopergolo LC, Lugao AB, Catalani LH. Polymer 2003;44:6217–22.
[17] Fechine GJM, Barros JAG, Catalani LH. Polymer 2004;45:4705–9.
[18] Fechine GJM, Barros JAG, Alcantara MR, Catalani LH. Polymer 2006;47:2629–33.
[19] Kadlubowski S, Henke A, Ulanski P, Rosiak JM, Bromberg L, Hatton TA. Polymer 2007;48:4974–81.
[20] D'Errico G, De Lellis M, Mangiapia G, Tedeschi A, Ortona O, Fusco S, et al. Biomacromolecules 2008;9:231–40.
[21] Petrov P, Petrova E, Tsvetanov CB. Polymer 2009;50:1118–23.
[22] Gaussian 03, Revision B.02. Pittsburgh PA: Gaussian, Inc.; 2003.
[23] Panarin EF, Kalninsh KK, Pestov DV. Euro Polym J 2001;37:375–9.
[24] Charlesby A, Pinner J. Atomic radiation and polymer. New York: Pergamon Press; 1960.
[25] Olejniczak J, Rosiak JM, Charlesby A. Radiat Phys Chem 1991;37:499–503. A computer program is available from Rosiak laboratory at. http://mitr.p.lodz.pl/biomat/gelsol.html.
[26] Krishnakumar V, Xavier RJ, Chithambarathanu T. Spectrochim Acta Part A 2005;62:931–9.
[27] Hassouna F, Therias S, Mailhot G, Gardette JL. Polym Degrad Stability 2009;94:2257–66.
[28] Dutta K, Brar AS. J Polym Sci Part A Polym Chem 1999;37:3922–8.
[29] Drago RS, Riley R. J Am Chem Soc 1990;112:215–8.
[30] Patton DE, Drago RS. J Chem Soc Perkin Trans. 1993;1:1611–5.
[31] Wang Y, Wang H. Radiat Phys Chem 2009;78:234–7.
[32] Gate EN, Hooper DL, Stevens MFG, Threadgill MD, Vaughan K. Magn. Reson. Chem. 1985;23:78–82.
[33] Laska B, Makarov GG, Sebenda J. Angew Makromol Chem 1992;196:143–54.
[34] Lanski B. Angew Makromol Chem 1997;252:139–51.
[35] Tang L, Sallet D, Lemaire J. Macromolecules 1982;15:1432–7.
[36] Roger A, Sallet D, Lemaire J. Macromolecules 1986;19:579–84.
[37] Sagar BF. J Chem Soc B 1967;428–39.
[38] Lemaire J. Pure Appl Chem 1982;54:1667–82.